Sparse polynomial surrogates for non-intrusive, high-dimensional uncertainty quantification of aerodynamic and aeroelastic computations

J.-L. Hantrais-Gervois[‡], **Éric Savin**[⋆,†]
jean-luc.hantrais-gervois@onera.fr
eric.savin@{onera,centralesupelec}.fr

[⋆] **ONERA – Information Processing & Systems Dept.**
8 chemin de la Hunière
F-91123 Palaiseau cedex, France

[‡] **ONERA – Aerodynamics Aeroelasticity Acoustics Dept.**
8 rue des Vertugadins
F-92190 Meudon, France

ONERA
THE FRENCH AEROSPACE LAB

[†] **CentraleSupélec – Engineering Mechanics Dept.**
8-10 rue Joliot-Curie
F-91190 Gif-sur-Yvette, France

CentraleSupélec

Some motivations...

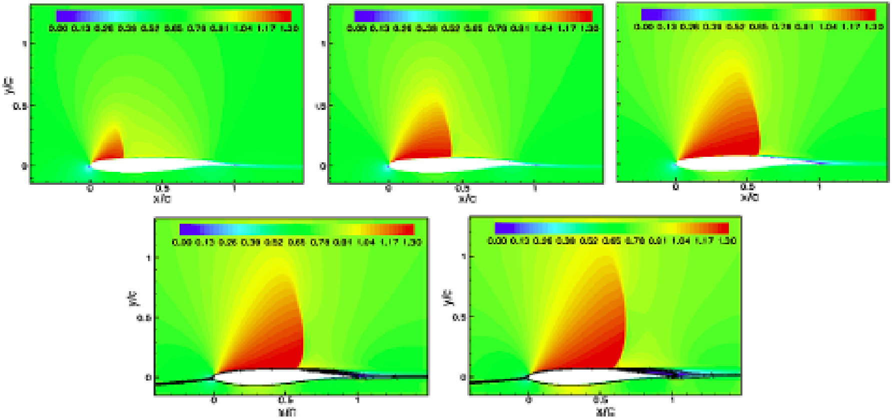

Mach number isocontour fields with 5 different inflow Mach number conditions ($\underline{M}_\infty = 0.73$) for an OAT15A profile: $0.92 \times \underline{M}_\infty$, $0.96 \times \underline{M}_\infty$, $\underline{M}_\infty$, $1.04 \times \underline{M}_\infty$, $1.08 \times \underline{M}_\infty$.

Simon-Guillen-Sagaut-Lucor, *Comput. Methods Appl. Mech. Engng.* **199**, 1091 (2010)

Overview

Overview

1. Background on UQ in CFD
2. Sparse reconstruction
3. Application to BC-02: RAE2822 transonic airfoil (2D)

Uncertainty Quantification in CFD – Model problem

- A generic computational model g involving d parameters $\boldsymbol{\xi} = (\xi_1, \xi_2, \dots \xi_d) \in \mathbb{R}^d$:

$$\mathcal{Y} \ni y = g(\xi_1, \xi_2, \dots \xi_d)\,.$$

- A polynomial surrogate model g_N of order N:

$$g \approx g_N(\boldsymbol{x}) = \arg \min_{\pi \in \mathbb{P}^p[\boldsymbol{x}]} \frac{1}{2} \int_{\mathbb{R}^d} |g(\boldsymbol{x}) - \pi(\boldsymbol{x})|^2 \mathcal{P}_{\boldsymbol{\Xi}}(\mathrm{d}\boldsymbol{x})\,,$$

  of which desired "convergence" $\mathbb{E}\{|g_N(\boldsymbol{\xi}) - g(\boldsymbol{\xi})|^2\} \to 0$ as $N \to \infty$ depends on $\mathcal{P}_{\boldsymbol{\Xi}}$ (and does not necessarily hold).

- Embedded projection (spectral stochastic finite elements), non-intrusive projection, "collocation", kriging, regression...

Non-intrusive UQ – Polynomial chaos (projection)

- Assume a (truncated) orthonormal basis $\mathcal{B}^N \equiv \{\psi_\alpha\}_{\alpha=0}^N$ of $L^2(\Omega, \mathcal{P}_{\boldsymbol{\Xi}})$ is available, s.t.:

$$\int_{\mathbb{R}^d} \psi_\alpha(\boldsymbol{x})\psi_\beta(\boldsymbol{x})\mathcal{P}_{\boldsymbol{\Xi}}(\mathrm{d}\boldsymbol{x}) = (\psi_\alpha, \psi_\beta)_{L^2} = \delta_{\alpha\beta}\,.$$

- Then $g_N = \sum_{\alpha=0}^N g_\alpha \psi_\alpha$ where $g_\alpha = (g, \psi_\alpha)_{L^2}$, $0 \leq \alpha \leq N$.
- But using the quadrature $\boldsymbol{\Theta}^M$, $g_N \simeq \sum_{\alpha=0}^N g_\alpha^M \psi_\alpha$ with:

$$g_\alpha^M = \sum_{\ell=1}^M \omega_\ell y_\ell \psi_\alpha(\boldsymbol{\xi}_\ell)\,, \quad 0 \leq \alpha \leq N\,.$$

- **Remark**: $\mathcal{P}_{\boldsymbol{\Xi}} = \otimes_{j=1}^d \mathcal{N}(0,1)$ is called polynomial chaos (PC), and generalized polynomial chaos (gPC) otherwise.

Non-intrusive UQ - Outcome

- Therefore we need:
  1. a quadrature rule in $\mathbb{R}^d$: $\boldsymbol{\Theta}^M \equiv \{\boldsymbol{\xi}_\ell, \omega_\ell\}_{\ell=\mathbf{1}}^M$;
  2. to perform repeated evaluations $\{y_\ell = g(\boldsymbol{\xi}_\ell)\}_{\ell=\mathbf{1}}^M$;
  3. to assess the accuracy of g_N (UQ-surrogate) independently of the accuracy of g (CFD solver).
- **Problem**: $M \gg 1$, and even $M \gg 100$, which is often unaffordable (and actually useless).

Overview

Compressed sensing

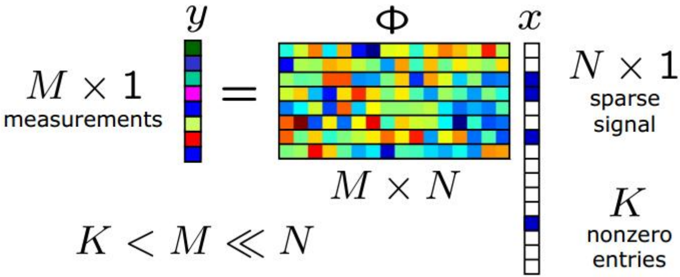

Candès-Romberg-Tao *Commun. Pure Appl. Math.* **59**(8), 1207 (2006)
Donoho *IEEE Trans. Inform. Theory* **52**(4), 1289 (2006)

Sparse reconstruction techniques – Principle

- Sparse polynomial decompositions *via* convex ℓ_1–minimization (Basis Pursuit Denoising, Chen-Donoho-Saunders 1998) whenever $M \ll N$ and only few coefficients g_α are non zero:

$$\boldsymbol{g}^\star = \arg\min_{\boldsymbol{g}\in\mathbb{R}^N} \{\|\boldsymbol{W}\boldsymbol{g}\|_1;\ \|\boldsymbol{y} - \boldsymbol{\Phi}\boldsymbol{g}\|_2 \leq \varepsilon\}\,. \qquad (P_{1,\varepsilon})$$

- Here $\boldsymbol{W}$ is some weighting, $\boldsymbol{g} = (g_0, g_1, \dots g_N)^\mathsf{T}$,

$$[\boldsymbol{\Phi}]_{\ell\alpha} = \psi_\alpha(\boldsymbol{\xi}_\ell)\,,$$

and the sampling points $\{\boldsymbol{\xi}_\ell\}_{\ell=1}^M$ should be selected s.t. the Vandermonde-type measurement matrix $\boldsymbol{\Phi}$ has maximum incoherence.

Definition (Coherence)

$$\mu(\boldsymbol{\Theta}^M, \mathcal{B}^N) = \max_{\substack{\mathbf{0} \leq \alpha \leq N \\ \mathbf{1} \leq \ell \leq M}} |\psi_\alpha(\boldsymbol{\xi}_\ell)|^2 \,.$$

Theorem (1)

Assume g_N is K-sparse on the gPC basis $\mathcal{B}^N$. Then if M measurements $\{\boldsymbol{\xi}_\ell\}_{\ell=1}^M$ are selected at random, and:

$$M \geq C \cdot \mu(\boldsymbol{\Theta}^M, \mathcal{B}^N) \cdot K \cdot \log N$$

for some $C > 0$, the solution to $(P_{1,0})$ is exact with overwhelming (sic) probability.

Remark: as a rule of thumb, $M \geq 4K$ is enough for a successful recovery.

Sparse reconstruction techniques – The theorems

Candès-Romberg-Tao (2006)

Definition (Restricted isometry constant)

The smallest number $\delta_K < 1$ s.t.:

$$(1-\delta_K)\|\boldsymbol{g}_K\|_2^2 \leq \|\boldsymbol{\Phi}\boldsymbol{g}_K\|_2^2 \leq (1+\delta_K)\|\boldsymbol{g}_K\|_2^2$$

for all K-sparse vectors $\boldsymbol{g}_K \in \mathcal{X}_K := \{\boldsymbol{g} \in \mathbb{R}^N;\ \|\boldsymbol{g}\|_0 \leq K\}$.

Theorem (2)

Assume $\delta_{2K} < \sqrt{2}-1$. Then the solution $\boldsymbol{g}^\star$ to $(P_{1,\varepsilon})$ satisfies:

$$\|\boldsymbol{g}^\star - \boldsymbol{g}\|_2 \leq C_0 \frac{\|\boldsymbol{g}_K - \boldsymbol{g}\|_1}{\sqrt{K}} + C_1\varepsilon$$

for some $C_0, C_1 > 0$ depending only on δ_{2K}.

Remark: the theorem allows to deal with imprecise measurements $\varepsilon > 0$ and approximately sparse vectors.

Overview

Numerical model

- RANS + Spalart-Allmaras model, $769c \times 193c$ mesh:

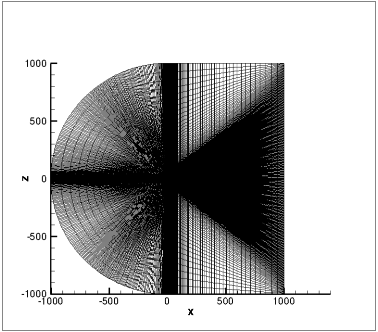

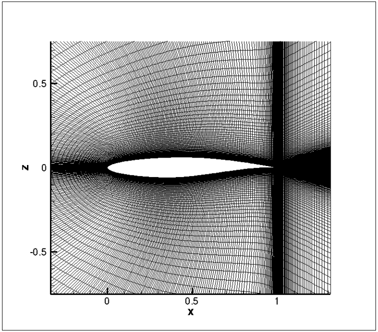

- Multigrid approach for the NS system over 3 grid levels with 2 iterations on the coarse grid and 1 fine level iteration for the turbulent equation.
- 2000 iterations with Roe flux and 2nd order MUSCL scheme for the convective term of the NS system.

Cambier-Heib-Plot *Mechanics & Industry* **14**(3), 159 (2013)

Nominal flow: $\underline{M_\infty} = 0.729$, $\underline{\alpha} = 2.31°$, $\underline{Re} = 6.50\,10^6$

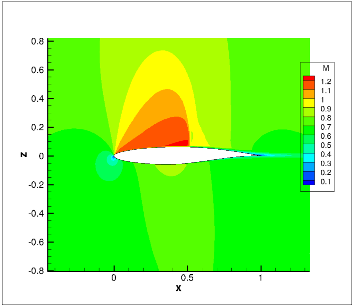

Velocity magnitude

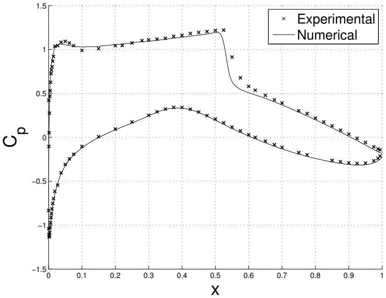

Static pressure coefficient C_p

- Shock wave well captured, good agreement with experiments (AGARD Report #AR-138 1979, NPARC Alliance Validation Archive 1998).
- Typical computational time: 2 hours.

Definition of the uncertainties ($d = 3$)

- The thickness-to-chord ratio $r \equiv \xi_1$, free stream Mach number $M_\infty \equiv \xi_2$, and angle of attack $\alpha \equiv \xi_3$ are $d = 3$ variable parameters following $\beta_{\mathrm{I}}(a, b)$ marginal probability laws.

	$a = b$	X_m	X_M
ξ_1	4	$0.97 \times \underline{r}$	$1.03 \times \underline{r}$
ξ_2	4	$0.95 \times \underline{M}_\infty$	$1.05 \times \underline{M}_\infty$
ξ_3	4	$0.98 \times \underline{\alpha}$	$1.02 \times \underline{\alpha}$

- **Remark**: $\xi \sim \beta_{\mathrm{I}}(a, b)$ arises from Jaynes' `MaxEnt` once (i) the compact support $[X_m, X_M]$ (ii) the means $\mathbb{E}\{\log(\xi - X_m)\}$ and $\mathbb{E}\{\log(X_M - \xi)\}$ are known.
- Our aim is to construct polynomial surrogates for the drag, lift and pitching moment coefficients C_D, C_L and C_m using gPC adapted to the foregoing PDFs (Jacobi polynomials).

Sampling sets (design of experiments DoE)

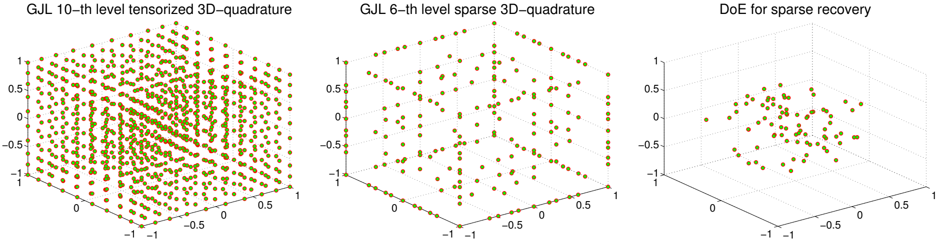

- The 1-dimensional Gauss-Jacobi quadrature $\mathbf{\Theta}_1^M$:

$$\int_{-1}^{1} f(x)(1-x)^a(1+x)^b \mathrm{d}x \simeq \sum_{\ell=1}^{M-M_b} \omega_\ell f(\xi_\ell) + \sum_{\ell'=1}^{M_b} \omega_{M-M_b+\ell'} f(\xi_{M-M_b+\ell'})$$

  is exact for polynomials up to order $2M-1-M_b$, where M_b is the number of fixed nodes (*e.g.* ± 1).
  - $M_b = 0$ is the classical Gauss-Jacobi (GJ) rule;
  - $M_b = 1$ is the Gauss-Jacobi-Radau (GJR) rule;
  - $M_b = 2$ $(-\xi_{N-1} = \xi_N = 1)$ is the Gauss-Jacobi-Lobatto (GJL) rule.
- Multi-dimensional quadratures may be obtained by tensorization and/or sparsification.

Sampling sets (design of experiments DoE)

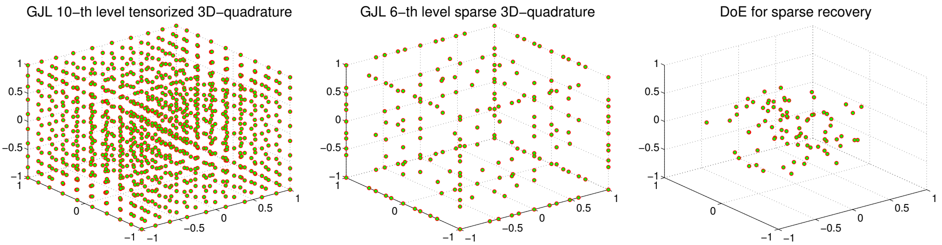

- k-th level d-dimensional sparse grid (Smolyak 1963):

$$\boldsymbol{\Theta}_{d,k}=\sum_{k+1\leq j_1+\cdots+j_d\leq k+d}\boldsymbol{\Theta}_1^{j_1}\otimes\cdots\otimes\boldsymbol{\Theta}_1^{j_d}\,.$$

- **Example**: $k=5$, $d=3$, then $M=99$ using a 1D GJL rule,

$$\boldsymbol{\Theta}_{3,5}=\boldsymbol{\Theta}_1^2\otimes\boldsymbol{\Theta}_1^2\otimes\boldsymbol{\Theta}_1^2+\boldsymbol{\Theta}_1^2\otimes\boldsymbol{\Theta}_1^2\otimes\boldsymbol{\Theta}_1^3+\boldsymbol{\Theta}_1^2\otimes\boldsymbol{\Theta}_1^3\otimes\boldsymbol{\Theta}_1^3+\text{perm.}$$

- The k-th level d-dimensional sparse rule based on GJL nodes is exact for d-dimensional polynomials of total order $2k-3$ (Novak-Ritter 1999, Heiss-Winschel 2008).

Sampling sets (design of experiments DoE)

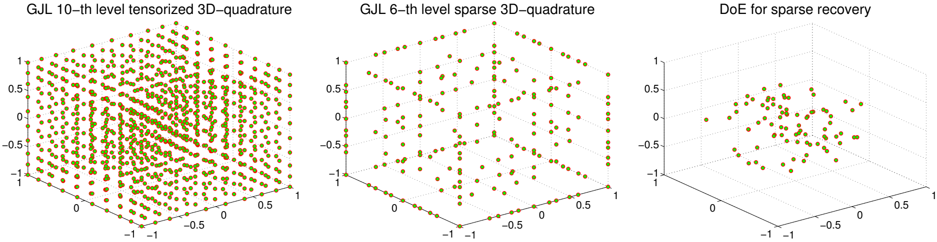

- Curse of dimensionality: $M = k^d$ for the product rule, while $M \sim \frac{(2d)^k}{k!}$ for the sparse rule with k fixed and $d \gg 1$.

k \ d	2	3	4	5	6
2	4	8	16	32	64
3	8	20	48	112	256
4	17	50	136	352	880
5	29	99	304	872	2384
6	53	201	673	2082	6092
7	85	363	1337	4483	14072
8	133	647	2585	9293	31025
9	193	1079	4697	18143	64469
10	273	1769	8321	34323	129197

- Sparse quadratures typically outperform product quadratures for $d \geq 4$.

Output statistics by 10–th level GJL product rule ($N = 165$, $M = 1000$)

- Mean/variance:

	μ	σ
C_D	133.37e-04	34.13e-04
C_L	72.274e-02	1.670e-02
C_m	-453.99e-04	32.24e-04

- PDFs:

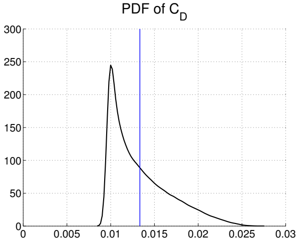

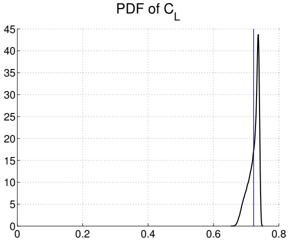

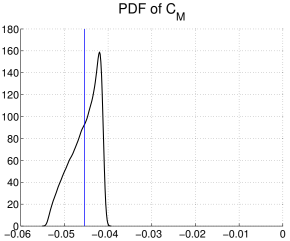

Output statistics by 6–th level GJL sparse rule ($N = 35$, $M = 201$)

- Mean/variance:

	μ	σ
C_D	133.38e-04	34.10e-04
C_L	72.269e-02	1.673e-02
C_m	-453.96e-04	32.18e-04

- PDFs:

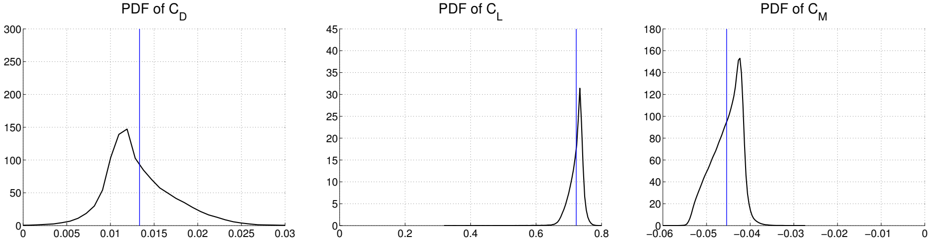

Output statistics by ℓ_1–minimization ($N = 165$, $M = 80$)

- Mean/variance:

	μ	σ
C_D	133.33e-04	34.05e-04
C_L	72.271e-02	1.670e-02
C_m	-453.95e-04	32.18e-04

- PDFs:

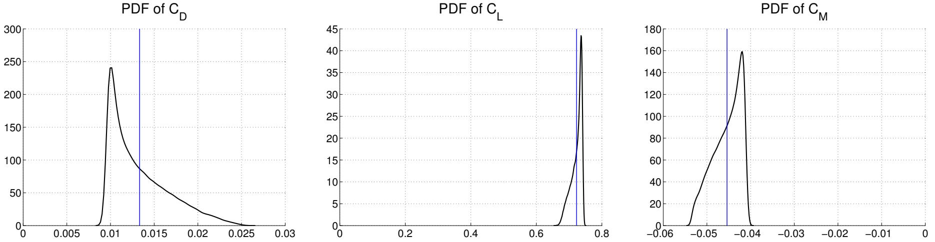

Summary

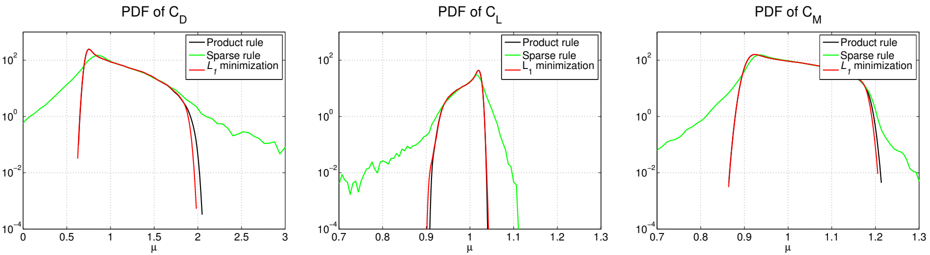

- Sparse recovery by ℓ_1–minimization assumes low-order interactions between the variable parameters;
- Sparsity can be proved for some parametric, possibly non-linear elliptic/parabolic PDEs (Chkifa-Cohen-Schwab 2014)–but for the present model it is rather observed *a posteriori*;
- Higher dimensions may be addressed alike–but invoking *e.g.* a McDiarmid inequality is that relevant?
- Optimal Uncertainty Quantification (Lucas-Owhadi-Ortiz 2008, Owhadi *et al.* 2013) to compute bounds of the probability of occurrence of a given critical scenario.

Numerical model

- RANS + Spalart-Allmaras model, $9,008,512$ cells:

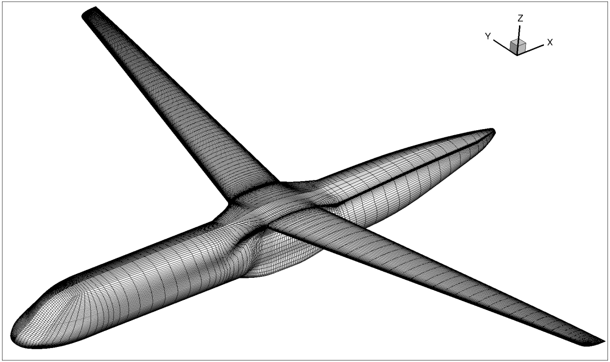

- Implicit LU-SSOR phase;
- Multigrid approach for the NS system over 3 grid levels;
- Jameson centered scheme with additional artificial viscosity outside of the boundary layers;
- Backward Euler time integration scheme;
- Typical computational time: 6 hours on 60 cores.

Cambier-Heib-Plot *Mechanics & Industry* **14**(3), 159 (2013)

Definition of the uncertainties ($d = 10$)

- The Mach number $M \equiv \xi_1$, lift coefficient $C_L \equiv \xi_2$, 4 wing bending parameters $\xi_3, \dots \xi_6$, and 4 wing torsion parameters $\xi_7, \dots \xi_{10}$ are $d = 10$ variable parameters following uniform marginal probability laws.

	X_m	X_M
ξ_1	0.74	0.76
ξ_2	0.55	0.65
$\xi_3 \dots \xi_6$	$0.5 \times \underline{I}$	$2.0 \times \underline{I}$
$\xi_7 \dots \xi_{10}$	$0.02 \times \underline{J}$	$10.0 \times \underline{J}$

- Our aim is to construct polynomial surrogates for the angle of attack α, drag coefficients C_{Ds} and C_{Dv} computed at the wing skin and in the far-field, respectively, pitching moment coefficient C_m, wing tip bend U, and wing tip twist ϕ using PC adapted to the foregoing PDFs (Legendre polynomials).

Sampling set (design of experiments DoE)

- The DoE is constituted by a combination of 18 manually generated sampling points (●) and 83 randomly generated sampling points (○) using Latin Hypercube Sampling (LHS).

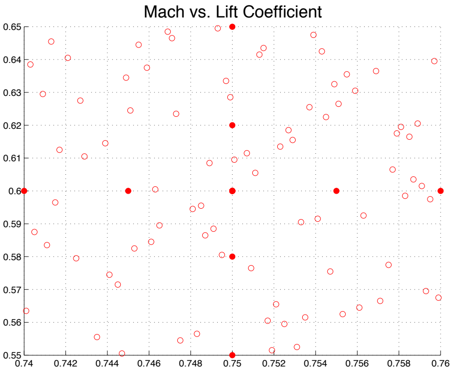

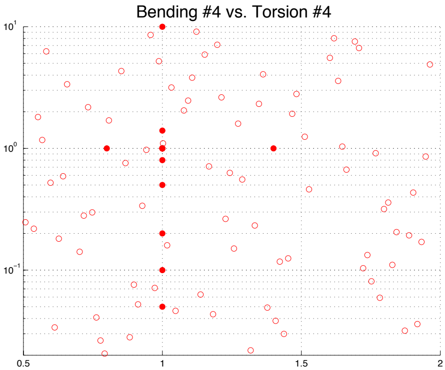

Output statistics by ℓ_1–minimization ($N = 285$, $M = 101$)

- Mean, variance, root-mean square error, and Kullback-Leibler divergence from a Normal distribution $\mathcal{N}$:

	C_m	C_{Ds}	C_{Dv}	α	U	ϕ
μ	**-11.63e-02**	**219.83e-04**	**218.69e-04**	**2.53**	**2.16**	**-6.10**
σ	**1.55e-02**	**6.53e-04**	**6.28e-04**	**0.20**	**0.26**	**0.80**
$e_{\mathbf{2}}$	**4.70e-03**	**0.45e-03**	**0.35e-03**	**1.88e-03**	**1.65e-03**	**3.97e-03**
$D_{\mathbf{KL}}(\mathcal{P}\|\|\mathcal{N})$	**1.10e-02**	**1.11e-02**	**1.39e-02**	**1.40e-02**	**0.50e-02**	**0.62e-02**

- PDFs:

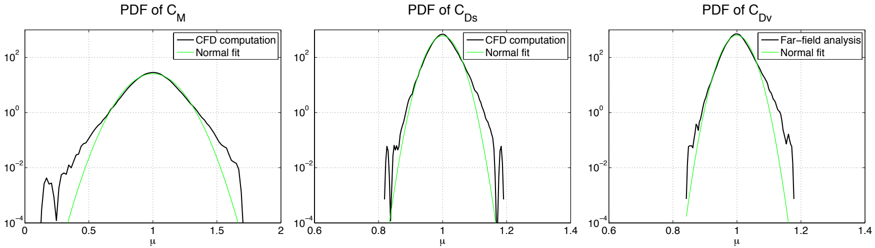

- Sensitivity to at most 2 or 3 parameters out of 10.

Output statistics by ℓ_1–minimization ($N = 285$, $M = 101$)

- Mean, variance, root-mean square error, and Kullback-Leibler divergence from a Normal distribution $\mathcal{N}$:

	C_m	C_{Ds}	C_{Dv}	α	U	ϕ
μ	-11.63e-02	219.83e-04	218.69e-04	2.53	2.16	-6.10
σ	1.55e-02	6.53e-04	6.28e-04	0.20	0.26	0.80
e_2	4.70e-03	0.45e-03	0.35e-03	1.88e-03	1.65e-03	3.97e-03
$D_{\mathbf{KL}}(\mathcal{P}\|\|\mathcal{N})$	1.10e-02	1.11e-02	1.39e-02	1.40e-02	0.50e-02	0.62e-02

- PDFs:

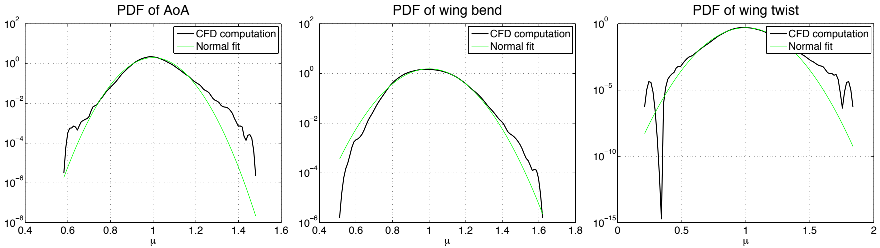

- Sensitivity to at most 2 or 3 parameters out of 10.

References

- G. Blatman, B. Sudret, *Prob. Engng. Mech.* 25(2), 183-197 (2010);
- E.J. Candès, J.K. Romberg, T. Tao, *IEEE Trans. Inform. Theory* 52(2), 489-509 (2006);
- E.J. Candès, M.B. Wakin, *IEEE Sig. Proc. Mag.* 25(2), 21-30 (2008);
- S. C. Chen, D. L. Donoho, M. A. Saunders, *SIAM J. Sci. Comput.* 20(1), 33-61 (1998);
- A. Chkifa, A. Cohen, C. Schwab, *J. Math. Pure Appl.* 103(2), 400-428 (2014);
- D.L. Donoho, *IEEE Trans. Inform. Theory* 52(4), 1289-1306 (2006);
- A. Doostan, H. Owhadi, *J. Comp. Phys.* 230(8), 3015-3034 (2011);
- J. Hampton, A. Doostan, *J. Comput. Phys.* 280, 363-386 (2015);
- J. Hampton, A. Doostan. Compressive sampling methods for sparse polynomial chaos expansions. In *Handbook of Uncertainty Quantification (R. G. Ghanem, D. Higdon, H. Owhadi eds.)*, Springer International Publishing, Cham (2016);
- F. Heiss, V. Winschel, *J. Econometrics* 144(1), 62-80 (2008);
- O. Le Maître, O. Knio. *Spectral Methods for Uncertainty Quantification. With Applications to Computational Fluid Dynamics*. Springer, Dordrecht (2010);
- L. Mathelin, K. A. Gallivan, *Commun. Comput. Phys.* 12(4), 919-954 (2012);
- F. Montomoli, M. Carnevale, A. D'Ammaro, M. Massini, S. Salvadori. *Uncertainty Quantification in Computational Fluid Dynamics and Aircraft Engines*. SpringerBriefs in Applied Sciences and Technology, Springer International Publishing, Cham (2015);
- E. Novak, K. Ritter, *Constructive Approx.* 15(4), 499-522 (1999);
- J. Peng, J. Hampton, A. Doostan, *J. Comput. Phys.* 267, 92-111 (2014); *J. Comput. Phys.* 310, 440-458 (2016);
- M. P. Pettersson, G. Iaccarino, J. Nordström. *Polynomial Chaos Methods for Hyperbolic Partial Differential Equations*. Springer International Publishing, Cham (2014);
- É. Savin, B. Faverjon, *Int. J. Num. Methods Engng.* 111(12), 1192-1200 (2017);
- É. Savin, A. Resmini, J. Peter, AIAA Paper #2016-0433 (2016);
- D. Schiavazzi, A. Doostan, G. Iaccarino, *Int. J. Uncertainty Quantification* 4(4), 303-331 (2014);
- C. Soize, R. Ghanem, *SIAM J. Sci. Comput.* 26(2), 395-410 (2004);
- E. van den Berg, M.P. Friedlander, *SIAM J. Sci. Comput.* 31(2), 890-912 (2008);
- L. Yan, L. Guo, D. Xiu, *Int. J. Uncertainty Quantification* 2(3), 279-293 (2012);
- X. Yuang, G. E. Karniadakis, *J. Comput. Phys.* 248, 87-108 (2013).

Acknowledgement

This work has been supported by the European Union's 7th Framework Program for research, technological development and demonstration under grant agreement #ACP3-GA-2013-605036.

UNCERTAINTY MANAGEMENT FOR ROBUST INDUSTRIAL DESIGN IN AERONAUTICS

UMRIDA

www.umrida.eu

Thank you for your attention!!